

Preservation of Geometrical Integrity of Supersolidus-Liquid-Phase-Sintered SKD11 Tool Steels Prepared with Powder Injection Molding

K.H. CHUANG and K.S. HWANG

The powder injection molded SKD11 tool steels often manifest shape retention problems during supersolidus liquid phase sintering due to the difficulties in controlling the amount of liquid phase. The typical temperature range for the sintering of SKD11 is only 10 K, between 1503 and 1513 K (1230 and 1240 °C), and this narrow sintering range demands a special furnace with very uniform temperature distribution. Through the addition of carbides, in particular TiC, this problem is resolved by enlarging the liquid + γ + carbide region in the phase diagram and by impeding the grain growth with the carbides. The resulting sintering window is broadened to 40 K, between 1513 and 1553 K (1240 and 1280 °C). The relevant mechanisms on the improvement of shape retention are discussed with a focus on the effect of carbide addition on the changes in the phase diagram and the microstructure. A guideline for the selection of effective carbides is also proposed based on the experimental results and the phase diagram analyses.

DOI: 10.1007/s11661-010-0593-8

© The Minerals, Metals & Materials Society and ASM International 2010

I. INTRODUCTION

POWDER Injection Molding is often applied in fabricating small components that have complicated shapes and high hardness, which make them difficult or costly to machine. Among the various PIM materials, tool steels are widely used for parts that require good wear resistance.^[1-3] One example is SKD11, used in the rotating cams in the hinges of notebook computers and mobile phones. It has a composition similar to that of D2 tool steels, as shown in Table I. Although SKD 11 has been widely used in the the PIM industry, complex-shaped parts made of SKD11 have suffered serious problems in dimensional control or even distortions.^[4-6] The main reason is that SKD11 compacts are generally consolidated through the supersolidus liquid phase sintering (SLPS) process, *i.e.*, sintering above the solidus line in the $L + \gamma + \text{carbide}$ or $L + \gamma$ region, as shown in Figure 1, where γ is the austenite, carbide is the M_7C_3 , and L is the liquid. To attain high sintered densities, the amount of liquid must be well controlled; if too much liquid is formed, then gravitational forces cause distortion or even slumping, while too little of the liquid amount will not densify the compact.^[7-9] Assuming that a successful sintering without distortion can be obtained with a liquid amount between 5 and 15 wt pct, this assumption leads to a very narrow temperature range of 1515 to 1523 K (1242 to 1250 °C), as shown in Figure 2. This small temperature range suggests that the amount of liquid is very sensitive to the temperature variation,

or the slope of the liquid fraction curve is steep, at about 1.25 wt pct/K. Thus, if SKD11 is sintered at 1520 K (1247 °C) with 10 wt pct liquid using a standard industrial sintering furnace with a guaranteed temperature uniformity of ± 10 K, the density will be too low for parts sintered in the solid state at 1510 K (1237 °C), while distortion will occur for parts sintered at 1530 K (1257 °C) because 18 wt pct liquid is present.

The above example demonstrates that when the solidus and liquidus lines in a phase diagram are flat and the temperature difference between these two lines is small, as shown in Figure 1 for SKD11, the amount of liquid becomes very difficult to control, for the lever rule indicates that a small temperature variation will result in large changes in the amount of the liquid phase. Figure 1 also indicates that higher carbon content decreases the optimal sintering temperature and enlarges the $L + \gamma + \text{carbide}$ phase region, which is beneficial for SLPS.^[10,11] However, the method of adding carbon is usually not practical because SKD11 has a specification for carbon, between 1.4 and 1.6 wt pct. To resolve the shape retention problem caused by the temperature sensitivity of the liquid content, Hachiga and Shiina mixed gas atomized powders of two different mean particle sizes with water atomized powders. The mixture with fine gas atomized powder showed a wider sintering window and improved mechanical properties.^[4] Nakayama *et al.* also demonstrated that gas atomized powders give higher sintered density, and the dimensional changes are less sensitive to the sintering temperature, compared to water atomized powders.^[5] To establish guidelines for a successful SLPS sintering, Liu *et al.* postulated that the dimensional control of SLPS products is closely related to the thickness of the liquid layer between adjacent particles, which is determined by the amount of liquid and the grain size.^[12]

K.H. CHUANG, Graduate Student, and K.S. HWANG, Professor, are with the Department of Materials Science and Engineering, National Taiwan University, Taipei 106, Taiwan, Republic of China. Contact e-mail: kshwang@ntu.edu.tw

Manuscript submitted July 1, 2010.

Article published online December 22, 2010

Table I. Compositions of SKD11 and D2 Tool Steels

Materials	Weight Percent							Standards
	C	Si	Mn	Cr	Mo	V	Other	
SKD11	1.40 to 1.60	0.40 max	0.60 max	11.00 to 13.00	0.80 to 1.20	0.20 to 0.50	Cu: 0.25 max	JIS G 4404:2006
D2	1.40 to 1.60	0.10 to 0.60	0.10 to 0.60	11.00 to 13.00	0.70 to 1.20	0.50 to 1.10	Ni + Cu: 0.75 max	ASTM A 681-08

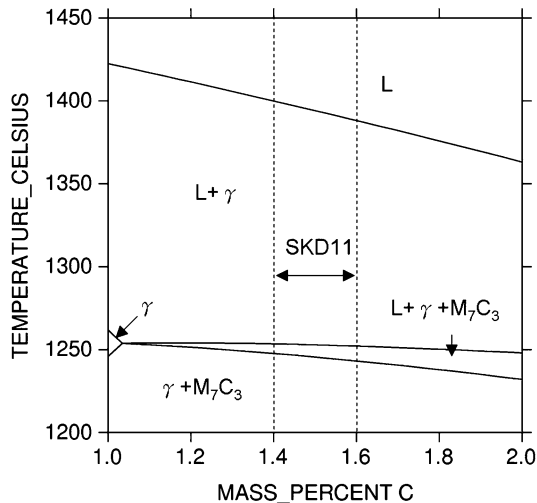


Fig. 1—Phase diagram of SKD11 (containing 1.4 to 1.6 wt pct carbon) calculated using Thermo-Calc software.

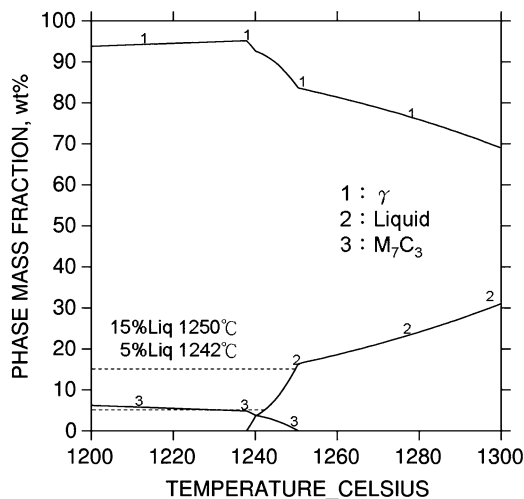


Fig. 2—Fractions of liquid, γ , and M_7C_3 in SKD11 showing that the amount of liquid is very sensitive to temperature variations between 1513 and 1523 K (1240 and 1250 °C).

To characterize whether a material is prone to distortion, they proposed a structure softening index ζ as follows:

$$\zeta = \frac{G^{1/3} V_L}{3 V_S} \quad [1]$$

where G is the grain size (μm), V_L is the volume fraction of the liquid, and V_S is the volume fraction of the solid.

This equation suggests that, with a fixed amount of liquid, finer grains provide larger grain boundary area and, thus, a thinner liquid layer between grains. As a result, particle sliding and particle rearrangement in the compact become difficult, and better shape retention can be attained.

Following this postulation, it is likely that different second phases, such as oxides, nitrides, and carbides, may provide the Zener pinning effect and inhibit the grain growth of tool steels and decrease the structure softening index ζ . Several previous studies have reported that some carbides, such as TiC and VC, are useful in inhibiting the grain size and enlarging the sintering window.^[13–20] However, not all carbides are effective, and different levels of success have been reported, depending on the baseline alloys and types of carbides. The M_7C_3 carbide in the SKD11 completely dissolves in the liquid phase at 1523 K (1250 °C), as shown in Figure 2. This high solubility of M_7C_3 carbide implies that grain growth becomes significant and the dimensional control becomes difficult above 1523 K (1250 °C), in the $L + \gamma$ region. Since the use of the theory proposed by Liu *et al.* on tool steels is still limited and the improvement on dimensional stability with the use of powders with different particle size or particle shape is modest, the objective of this study was thus to examine the effects of second phases, in particular carbides, on the preservation of the geometrical integrity of injection molded SKD11 tool steels. In this study, four different carbides, TiC, NbC, WC, and Cr_3C_2 , were tested to determine their effects on grain growth, densification, and shape retention of sintered compacts. The results are discussed with the focus on the solubility of the carbides in the matrix with the help of phase diagrams calculated using the Thermo-Calc software.

II. EXPERIMENTAL PROCEDURE

Water atomized SKD11 powder was used as the base powder in this study. The characteristics of the powder are shown in Table II. Since the powder contained 0.22 wt pct oxygen, which reacts with carbon during sintering and reduces the final carbon content to a level lower than the minimum specification of 1.4 wt pct, supplementary 0.25 wt pct graphite powder was added in the kneading process to meet the specification of 1.40 to 1.60 wt pct after sintering. To inhibit grain growth, TiC, NbC, WC, and Cr_3C_2 were also added during kneading. In the preliminary phase of the study, a screening test of using 2 vol pct of the four carbides was

Table II. Characteristics of Water Atomized SKD11 Tool Steel Powders

Composition (wt pct)	C1.52, Si0.32, Mn0.43, Ni0.10, V0.38, Cr12.02, Mo1.01, O0.22, Fe: bal
Pycnometer density (g/cm ³)	7.68
Particle size (μm)	D ₁₀ : 4.3 D ₅₀ : 11.7 D ₉₀ : 27.8
Shape	irregular
Designation	PF-20F
Supplier	Epson Atmix (Hachinohe, Japan)

Table III. Characteristics of Graphite and Carbide Powders

	Graphite	TiC	NbC	WC	Cr ₃ C ₂
Pycnometer density (g/cm ³)	2.45	4.9	7.67	15.48	6.59
Mean particle size (μm)	9.3	2.4	3.9	2.5	4.1
Supplier	Asbury Carbon (Asbury, NJ)	Changsha Wing High (Changsha, China)	Changsha Wing High (Changsha, China)	Xiamen Golden Egret (Xiamen, China)	Changsha Wing High (Changsha, China)

carried out, and the carbide with the best performance was selected for further study. The characteristics of the carbide and graphite powders are given in Table III.

To prepare PIM specimens, the powders were kneaded with a wax-based binder using a kneader with Σ-shaped blades. The kneaded feedstock was injection molded into tensile test specimens (MPIF Standard No. 50) and rectangular plates, 100 mm × 10 mm × 2 mm, using an injection molding machine (Arburg, 320C, 500-100, Lossburg, Germany). Molded specimens were immersed in 313 K (40 °C) heptane for 24 hours to remove the soluble binder. The remaining binder was thermally removed by heating specimens at a rate of 2 K/min to 1073 K (800 °C) in a tube furnace under hydrogen. The binder-free specimens were then sintered for 1 hour between 1473 and 1553 K (1200 and 1280 °C) using a vacuum furnace. The vacuum was controlled between 0.7 and 1 torr using argon as the backfilled gas to prevent chromium evaporation. After sintering, specimens were furnace cooled to 1073 K (800 °C) and then fan cooled to room temperature. The cooling rate measured at 673 K (400 °C) was about 30 K/min. The uniformity of the sintering temperature in the selected sintering zone was ±3 K at 1523 K (1250 °C) using temperature-control rings (STH, Ferro Electronic Materials, UDEN, Netherlands). To attain the desired mechanical properties, sintered compacts were heated to 1373 K (1100 °C) and held at that temperature for 10 minutes, followed by air cooling. The compacts were then cryogenically cooled at 77 K (-196 °C) for 30 minutes and then tempered twice for 2 hours each at either 473 or 793 K (200 or 520 °C).

The sintered density was measured using the Archimedes method, following MPIF Standard 54. For

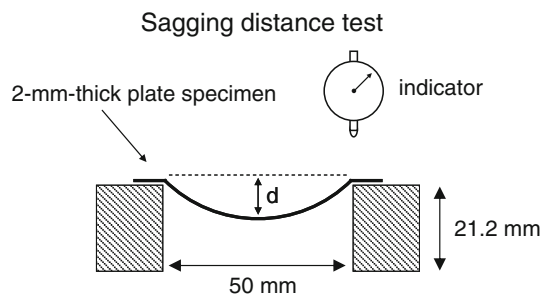


Fig. 3—Schematics of the setup for measuring the sagging distance of sintered specimens.

microstructure examination, the sintered compact was ground, polished, and etched with Vilella's Reagent (1 g picric acid, 5 mL HCl, and 100 mL alcohol). The etched specimens were examined under an optical microscope and a scanning electron microscope (JSM-6500F, JEOL*) equipped with an energy dispersive spectrum

*JEOL is a trademark of Japan Electron Optics Ltd., Tokyo.

(EDS) analyzer. An electron probe microanalyzer (EPMA, JXA-8200SX, JEOL) was also used to examine the distribution of elements. The grain size was measured using the line intercept method, following the ASTM E112-96 standard. To determine the sintering window, the lower limit was set to the temperature where a sintered density of 95 pct or 7.32 g/cm³ can be achieved. The upper limit was determined by the sagging distance, using the setup shown in Figure 3. When the sagging distance was over 12.5 mm, which was the value obtained for the SKD11 +0.25 wt pct carbon sintered and warped, the specimen was considered distorted.

In terms of mechanical properties, the hardness of the sintered specimen was measured using a Rockwell Hardness tester (ARK-600, Mitutoyo Co., Kanagawa, Japan). The tensile strength was measured using a Universal Tensile Tester (AG-10TE, Shimadzu Co., Kyoto, Japan). To check whether decarburization occurred, and to what extent, during sintering, thus influencing the mechanical properties, the carbon content was determined using a carbon analyzer (EMIA-220V, Horiba, Kyoto, Japan). The nitrogen and oxygen contents were also measured using an oxygen/nitrogen analyzer (TC-136, LECO Co., St. Joseph, MI).

To explain the experimental results, the phase diagrams of SKD11 tool steels with the composition shown in Table II, and the SKD11 tool steels with carbide additives, were calculated using Thermo-Calc software (Thermo-Calc Software, Stockholm) and a TCFE 3 database (TCS Steels/Fe-Alloys Database version 3). The fractions of the phases present were calculated and were correlated to the dimensional stability and the sintering window.

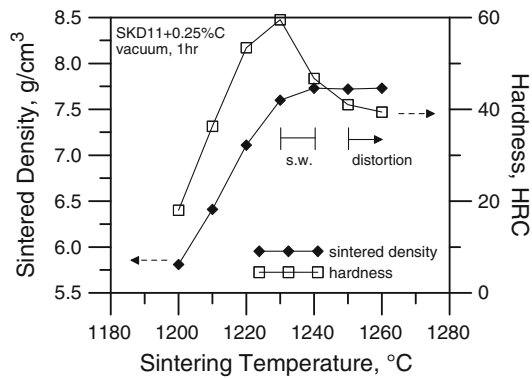


Fig. 4—Density and hardness of SKD11+0.25 wt pct carbon sintered between 1473 and 1533 K (1200 and 1260 °C) for 1 h.

III. RESULTS

To verify that the sintering window of SKD11 is quite narrow, as generally recognized, Figure 4 shows the density and hardness of the compacts sintered between 1473 and 1533 K (1200 and 1260 °C). These specimens contained 0.25 wt pct extra graphite to compensate for the carbon loss due to the reaction between carbon and the oxide or dissolved oxygen in the as-received powder. The final carbon content after sintering was 1.53 wt pct, within the specification of 1.40 to 1.60 wt for SKD11. As the temperature increased from 1473 to 1503 K (1200 to 1230 °C), the density increased from 5.81 g/cm³ (75.4 pct of the pore-free density of 7.70 g/cm³) to 7.60 g/cm³ (98.7 pct). The hardness also increased correspondingly to 60 HRC. As the temperature continued to increase, the density leveled off, while the hardness decreased. It was observed that the compact distorted when the temperature reached 1523 K (1250 °C). These results confirmed that the sintering window of the SKD11 was quite narrow, between 1503 and 1513 K (1230 and 1240 °C).

Figure 5 shows the microstructure of the SKD11+0.25 wt pct carbon compact. When sintered at 1493 K (1220 °C), many pores were present, and the white particles of M₇C₃ carbides, as identified using the EDS, were dispersed within the grain and along the grain boundaries. When sintered at 1503 K (1230 °C), far

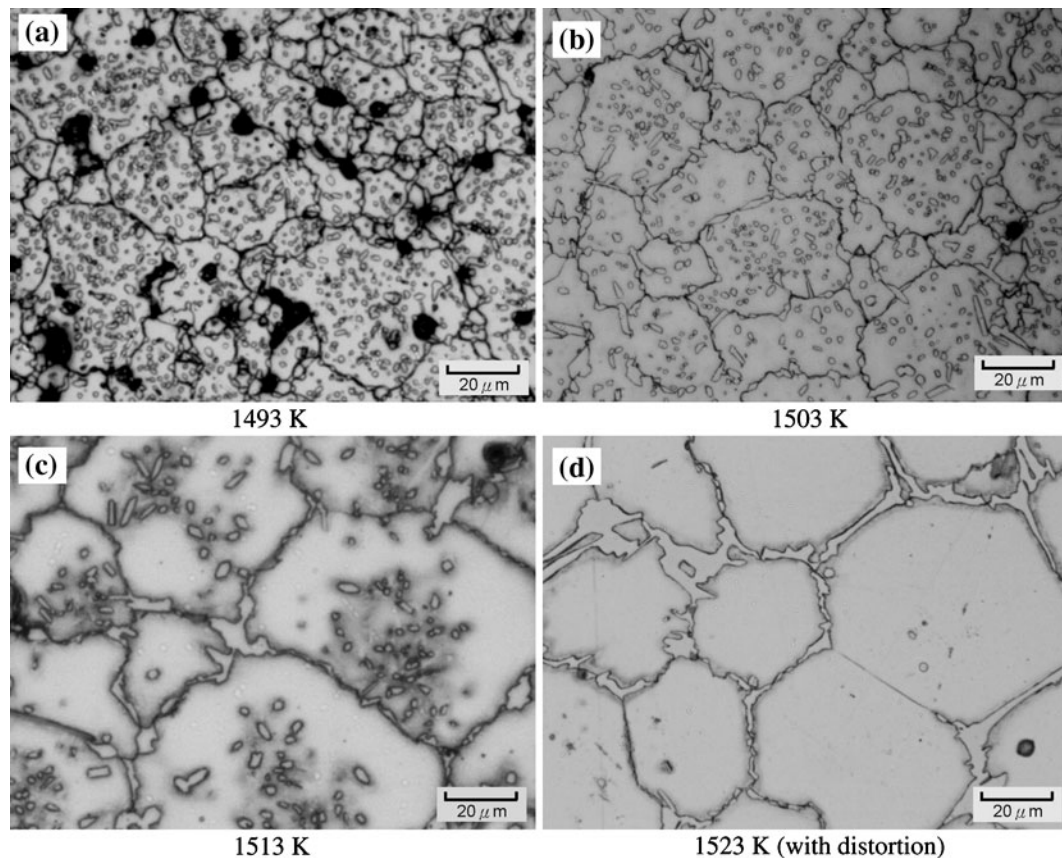


Fig. 5—Microstructure of SKD11+0.25 wt pct carbon sintered between 1493 and 1523 K (1220 and 1250 °C) for 1 h: (a) 1493 K (1220 °C), no distortion; (b) 1503 K (1230 °C), no distortion; (c) 1513 K (1240 °C), no distortion; and (d) 1523 K (1250 °C), with distortion.

fewer pores were present, and the M_7C_3 carbides were still uniformly distributed in the matrix. As the temperature further increased to 1513 K (1240 °C), grain growth became obvious and carbides near the grain boundaries disappeared. With larger grains and fewer carbides in the matrix, the hardness decreased, as shown in Figure 4. With sintering at 1523 K (1250 °C), very few carbides were observed inside the grain, while a continuous carbide network formed at grain boundaries. At this temperature, grain coarsening was significant and distortion was observed.

To impede grain growth and decrease the structure softening index ζ in Eq. [1], 2 vol pct carbides, TiC, NbC, WC, and Cr_3C_2 , were mixed into SKD11 powder, and their effects on sintered density, microstructure, and hardness were examined. The mixture of SKD11 and carbide powder, without graphite additions, was compacted and then sintered at 1523 K (1250 °C), which is higher than the upper limit of the sintering window of SKD11+0.25 wt pct carbon. Table IV shows that the carbon content of all specimens remained within the specification after being sintered at 1523 K (1250 °C) for 1 hour. Among the four carbides examined, Cr_3C_2 reached a density of 98.6 pct, while the rest of the carbides were about 99.6 pct. In terms of grain size, Cr_3C_2 was the least effective on inhibiting grain growth, while TiC was the best. To verify which carbides were more stable, the microstructures were examined under SEM using the backscattered electron mode. Figure 6 shows that little M_7C_3 was present inside the grains of SKD11+0.25 wt pct carbon compact. When TiC and NbC were added, these carbides remained undissolved inside the grain. In contrast, WC and Cr_3C_2 disappeared in the matrix and lost their roles of impeding the grain growth. These results of density, grain size, and microstructure suggest that TiC is the most stable carbide at the sintering temperature and the one least soluble in the matrix. These preliminary screening tests showed that TiC gave high sintered density and small grains without distortion. Thus, it was chosen for further detailed study in the subsequent experiments using different amounts of TiC and different sintering temperatures.

Figure 7 shows the effect of TiC amount on the carbon content and the grain size of the compact sintered at 1523 K (1250 °C) for 1 hour. For TiC-free and SKD11+0.5 wt pct TiC powders, 0.25 and 0.125 wt pct graphite powders were added, respectively, to keep the carbon content above the lower limit of 1.4 wt pct after sintering. However, for SKD11+1.0 to

3.0 wt pct TiC, no extra graphite powder was added. The results showed that the grain size was reduced significantly for the first 1 wt pct TiC addition, and then with decreasing effectiveness for further additions of TiC. When the TiC content was increased to 2 wt pct, the grain size decreased to 45 μm . Since 2 wt pct TiC has a positive grain refinement effect and its carbon content was 1.68 wt pct, only slightly above the 1.6 wt pct limit of SKD11, the SKD11+2 wt pct TiC was selected for the subsequent experiments to determine the sintering window and the resulting mechanical properties.

Figure 8 shows the sintered density and hardness of SKD11+2 wt pct TiC compact sintered between 1483 and 1563 K (1210 and 1290 °C) for 1 hour. As the temperature increased to 1513 K (1240 °C), the compact reached a density above 7.62 g/cm^3 or 99.2 pct. As the temperature continued to increase, the density leveled off, but distortion occurred at 1563 K (1290 °C). Thus, the sintering window was determined to be 1513 to 1553 K (1240 to 1280 °C), which is 4 times wider than the 1503 to 1513 K (1230 to 1240 °C) of the TiC-free SKD11, as shown in Figure 4. Figure 8 also indicates that, once the compact was densified above 1513 K (1240 °C), the hardness started to decrease with further increases in the sintering temperature due to the grain growth and the decrease in the amount of carbide in the matrix, similar to that observed in the TiC-free SKD11.

To explain how TiC improved the shape retention capability, the microstructure of the SKD11+2 wt pct TiC was examined, as shown in Figure 9. The liquid was observed at grain boundaries when the compact was sintered at 1513 K (1240 °C). The white M_7C_3 carbides were still present inside the grain. However, the TiC evolved into gray (Ti,V)C carbide during sintering, as was identified with the EPMA. As the temperature increased to 1523 K (1250 °C), most M_7C_3 carbides in the matrix disappeared, while some (Ti,V)C remained in the matrix, and the amount of liquid increased and formed continuous networks, which could have adverse effects on ductility. When compacts were sintered at 1533 K (1260 °C), the amount of liquid continued to increase and the liquid layer thickened.

In addition to the visual observation for slumping, sagging distance was also measured as a quantitative method in determining the distortion. Figure 10 shows the sagging distance of the SKD11+0.25 wt pct carbon and SKD11+2 wt pct TiC compact sintered between 1483 and 1563 K (1210 and 1290 °C). The amount of

Table IV. Effect of 2 Vol pct Carbide Addition on the Density and Grain Size of SKD11 Sintered at 1523 K (1250 °C) in Vacuum for 1 h

Additive	Mean Carbide Particle Size (μm)	Carbon (wt pct)	Sintered Density (g/cm^3 (Pct))	Grain Size (μm)	Hardness (HRC)
+0.25 wt pct carbon	—	1.53	7.69 (99.9)	117	38
+2 vol pct (1.71 wt pct) Cr_3C_2	4.1	1.60	7.57 (98.6)	104	38
+2 vol pct (3.98 wt pct) WC	2.5	1.57	7.83 (99.6)	98	41
+2 vol pct (1.99 wt pct) NbC	3.9	1.59	7.68 (99.7)	80	39
+2 vol pct (1.27 wt pct) TiC	2.4	1.56	7.65 (99.6)	68	42

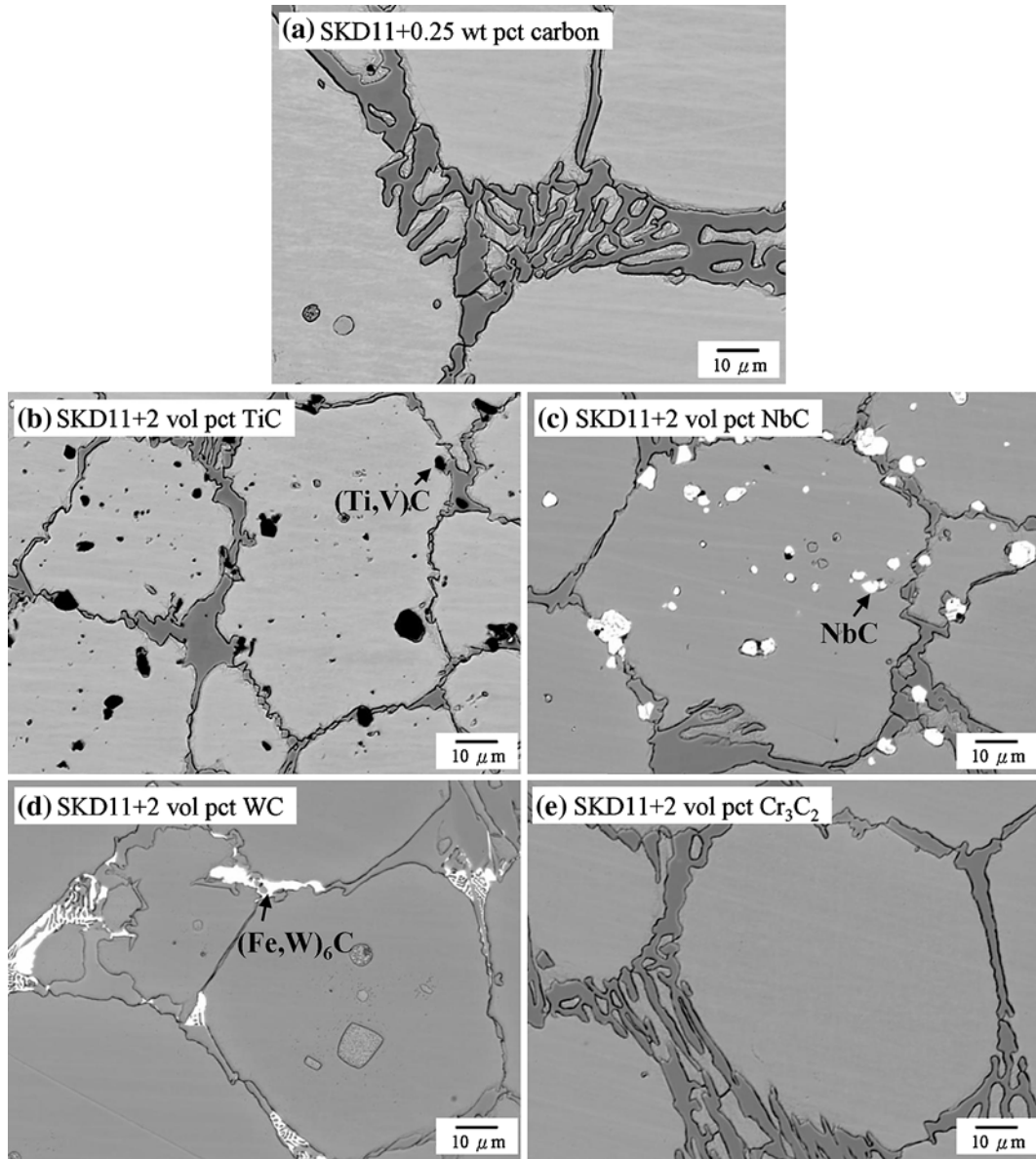


Fig. 6—Backscattering electron micrographs of SKD11 sintered at 1523 K (1250 °C) for 1 h: (a) +0.25 wt pct carbon, (b) +2 vol pct TiC, (c) +2 vol pct NbC, (d) +2 vol pct WC, and (e) +2 vol pct Cr₃C₂.

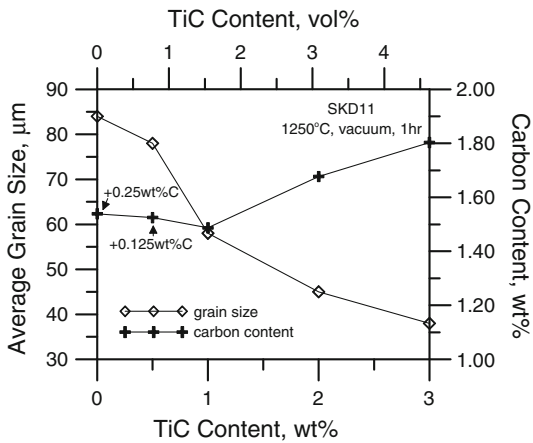


Fig. 7—Influence of TiC on the grain size and the total carbon content.

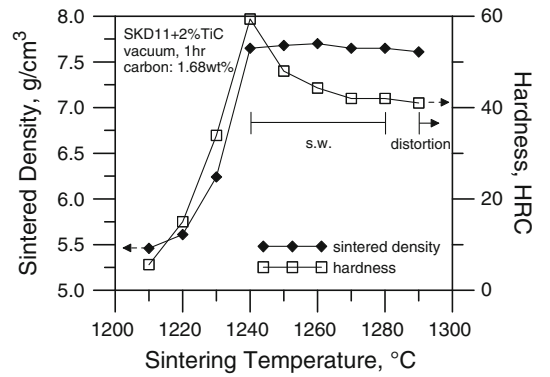


Fig. 8—Density and hardness of SKD11+2 wt pct TiC sintered between 1483 and 1563 K (1210 and 1290 °C) for 1 h, showing that the sintering window is 1513 to 1553 K (1240 to 1280 °C).

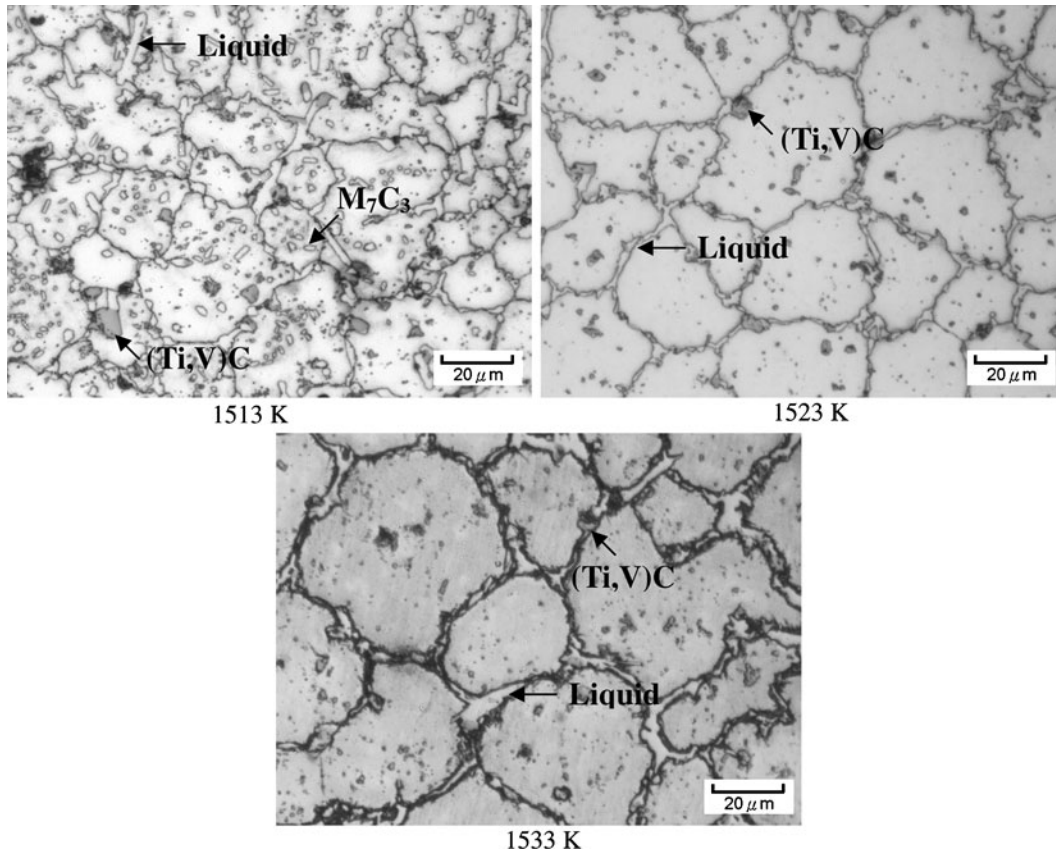


Fig. 9—Microstructure of the SKD11+2 wt pct TiC sintered at 1513, 1523, and 1533 K (1240, 1250, and 1260 °C) for 1 h without distortion.

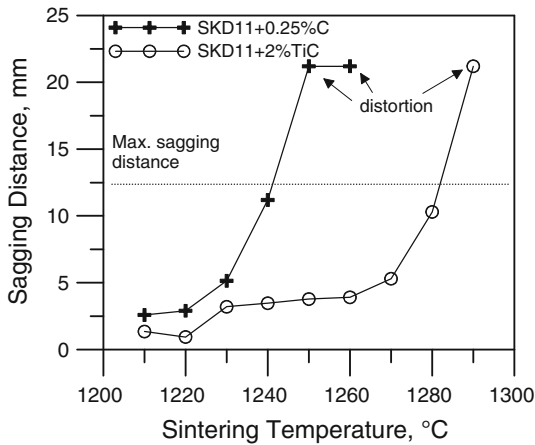


Fig. 10—Sagging distance of SKD11+0.25 wt pct carbon and SKD11+2 wt pct TiC sintered between 1483 and 1563 K (1210 and 1290 °C).

sagging of SKD11+0.25 wt pct carbon started to increase significantly at 1503 K (1230 °C), and the compact slumped at 1523 K (1250 °C). The corresponding sagging distances were 5.2 and 21.2 mm, respectively. In contrast, with 2 vol pct TiC addition, only slight sagging was observed between 1483 and 1543 K (1210 and 1270 °C). However, at 1553 K (1280 °C), the sagging distance increased significantly to 10.3 mm.

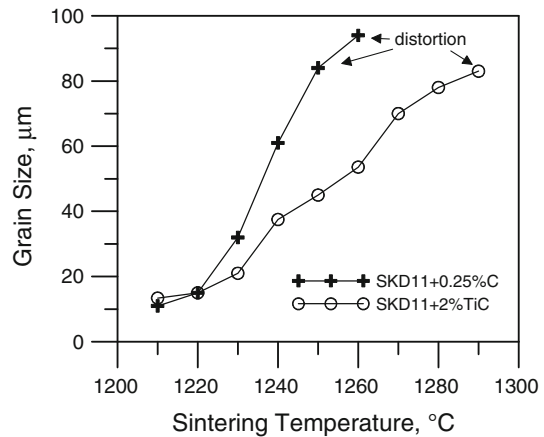


Fig. 11—Effect of TiC addition on the grain size of SKD11 sintered between 1483 and 1563 K (1210 and 1290 °C).

Figure 11 shows the grain sizes of the SKD11+0.25 wt pct carbon and SKD11+2 wt pct TiC compacts. When sintered at 1493 K (1220 °C), the grain sizes of both compacts were about 15 μm . As the temperature increased, the grain sizes of the TiC-free compacts sintered at 1523 and 1533 K (1250 and 1260 °C) were 83 and 95 μm , respectively. In comparison, with 2 wt pct TiC addition, the grain growth was

Table V. Comparison of Hardness and Tensile Strength of SKD11 before and after Heat Treatment

Additive	Hardness (HRC)			Ultimate Tensile Strength (MPa) (Standard Deviation)		
	As Sintered	473 K (200 °C) Twice	793 K (520 °C) Twice	As Sintered	473 K (200 °C)	793 K (520 °C)
+ 0.25 wt pct carbon	53	62	59	1159 (244)	1206 (163)	1482 (132)
+ 1 wt pct TiC	55	62	58	1309 (120)	1309 (109)	1767 (177)
+ 2 wt pct TiC	54	62	58	1215 (81)	1600 (164)	1760 (56)

Sintering: 1513 K (1240 °C), 1 h, vacuum.
 Hardening: 1373 K (1100 °C), 10 min, air cooling.
 Cryogenic treatment: 77 K (-196 °C), 30 min.
 Tempering: 473 K (200 °C), 2 h, or 793 K (520 °C), 2 h.

impeded, and the grain size of the compact sintered at these two temperatures was less than 60 μm. Only when the temperature increased to 1563 K (1290 °C) was distortion noticed. The grain size of this compact was 82 μm. The grain sizes of the compacts that contain 10 wt pct liquid were also used for the calculation of the structural softening index. The corresponding indices were 0.16 and 0.14 for the SKD11 + 0.25 wt pct carbon and SKD11 + 2 wt pct TiC, respectively. The larger index of the TiC-free specimen suggested that it was more likely to distort.

The main reason for the wide application of SKD11 is its high hardness and strength. Table V shows that the TiC addition slightly increased the hardness in the as-sintered compact. But after cryogenic cooling and tempering at 473 K (200 °C) for 2 hours twice, all compacts, with or without TiC addition, reached 62 HRC. When tempered twice at 793 K (520 °C) for 2 hours, the hardness decreased slightly to about 58 HRC. These hardness results were similar to those of the wrought products. In terms of the ultimate tensile strength, both the TiC addition and heat treatment increased the strength. However, a little elongation, less than 1 pct, was obtained on all specimens, most likely caused by the continuous carbide network.

The results given in the previous sections suggest that the addition of TiC can effectively decrease the grain size and prevent distortion. With 2 wt pct TiC addition, the sintering window can be broadened to 1513 to 1553 K (1240 to 1280 °C). Within this range, the compact can achieve a density greater than 7.62 g/cm³, or 99.2 pct, without distortion, and the grain size can be controlled to 78 μm or less.

IV. DISCUSSION

To explain how the TiC additive helps improve the shape retention of SKD11 compacts, the Thermo-Calc software was used to calculate the phase diagram of the SKD11 + 1.6 wt pct Ti + 0.4 wt pct carbon, which has the same composition as SKD11 + 2 wt pct TiC. As shown in Figure 12, the TiC transforms into (Ti,V)C in the temperature range used in this study, from 1473 to 1573 K (1200 to 1300 °C). The figure also shows that as the temperature reaches 1522 K (1249 °C), liquid starts to form and increases in amount at a very fast rate as the

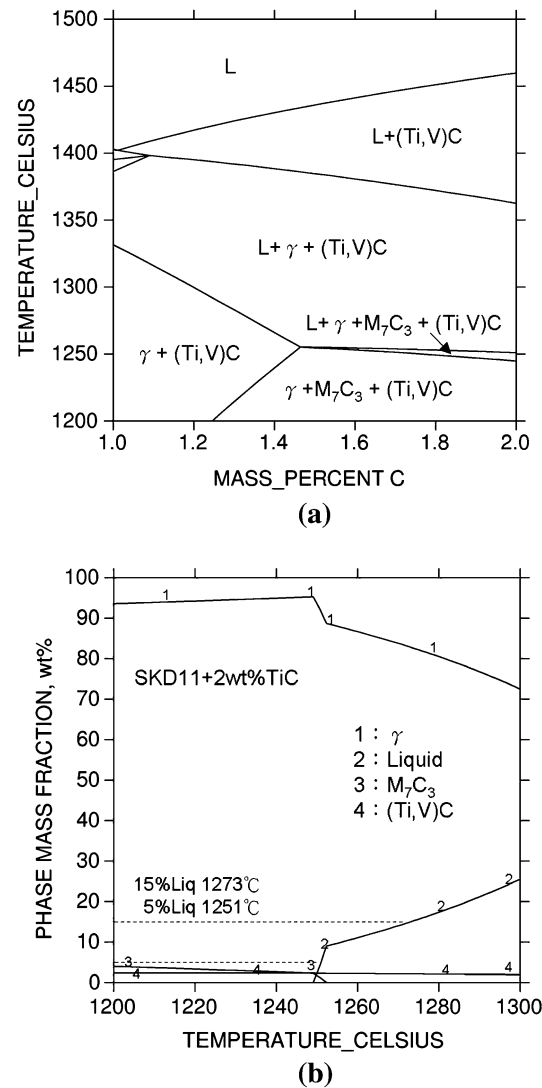


Fig. 12—(a) Phase diagram of SKD11 + 2 wt pct TiC calculated with Thermo-Calc software, (b) The amount of liquid, γ, M₇C₃, and (Ti,V)C in SKD11 between 1473 and 1573 K (1200 and 1300 °C).

temperature increases. Meanwhile, the M₇C₃ becomes completely dissolved in the matrix at 1525 K (1252 °C). The temperature range for the supersolidus liquid phase sintering that contains carbides, either M₇C₃ or (Ti,V)C, has become quite wide, between 1522 and 1656 K (1249

and 1383 °C), which is much larger than the 1511 to 1523 K (1238 to 1250 °C) of the standard SKD11, as shown in Figure 2. Since M_7C_3 or (Ti,V)C can inhibit grain growth, the distortion problem of SKD11 can be alleviated.

It can be argued that the sintering window obtained experimentally, between 1503 and 1513 K (1230 and 1240 °C), is lower than the temperature range of 1511 to 1523 K (1238 to 1250 °C), where both liquid and carbides coexist in the calculated phase diagram. This phenomenon is not unexpected, as the prealloyed SKD11 powder is not completely homogeneous due to the slow cooling rate of the atomization process. With impurities segregated at the grain boundaries, liquid will form at a lower melting temperature, reaching as much as 25 K for atomized powders.^[7] With this understanding, the use of the calculated phase diagram, which is established under equilibrium conditions, for the explanation of the experimental results should be acceptable.

In addition to enlarging the temperature range that contains carbides, the other condition that helps retain the geometrical integrity of SKD11 is to reduce the sensitivity of the liquid amount to temperature. The standard SKD11 has a very steep slope of the liquid

fraction, as shown in Figure 2. Assuming that the maximum amount of liquid allowed for a successful SLPS is 15 wt pct, which occurs at 1523 K (1250 °C), while the minimum amount of liquid required to densify the green compact is 5 wt pct, which occurs at 1515 K (1242 °C), the average rate of change for the amount of liquid in this temperature range is 1.25 wt pct/K. When 2 wt pct TiC was added, the average slope decreased to 0.45 wt pct/K, as shown in Figure 12(b).

To test whether these two criteria also applied to other carbides, the phase diagrams of the SKD11 samples that were doped with 2 vol pct NbC, WC, or Cr_3C_2 were also calculated. As shown in Figure 13, WC and Cr_3C_2 produce phase diagrams similar to that of the standard SKD11, while NbC broadens the $L + \gamma +$ carbide region. Figure 13 further shows that NbC is present between 1473 and 1673 K (1200 and 1400 °C). Thus, as M_7C_3 dissolves completely in the matrix or liquid at 1522 K (1249 °C), NbC remains in the material and acts as a grain growth inhibitor. In contrast, the temperature ranges where the liquid and carbide co-exist are 1497 to 1513 K (1224 to 1240 °C) and 1519 to 1531 K (1246 to 1258 °C), for WC and Cr_3C_2 , respectively. These phase diagrams predict that

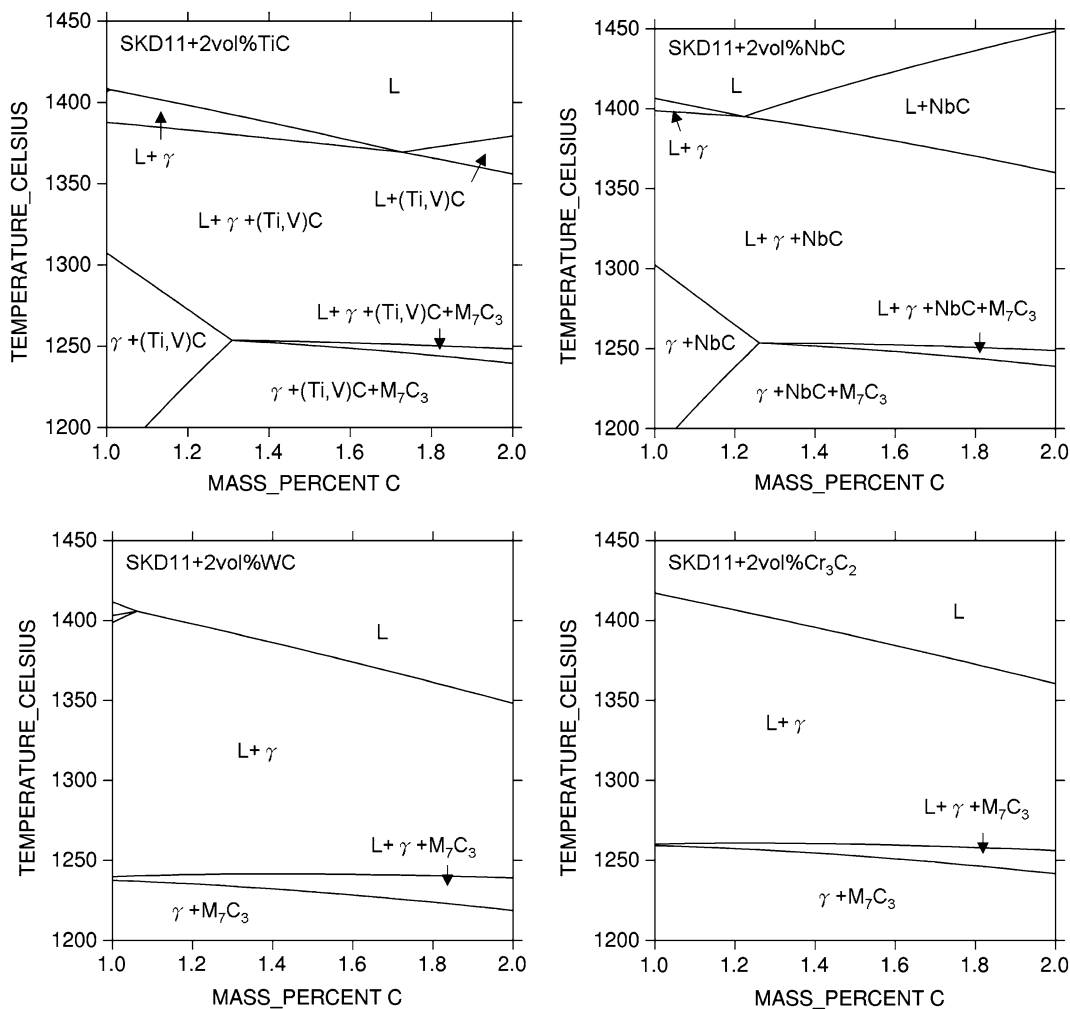


Fig. 13—Phase diagram of SKD11+2 vol pct TiC, NbC, WC, and Cr_3C_2 calculated with the Thermo-Calc software.

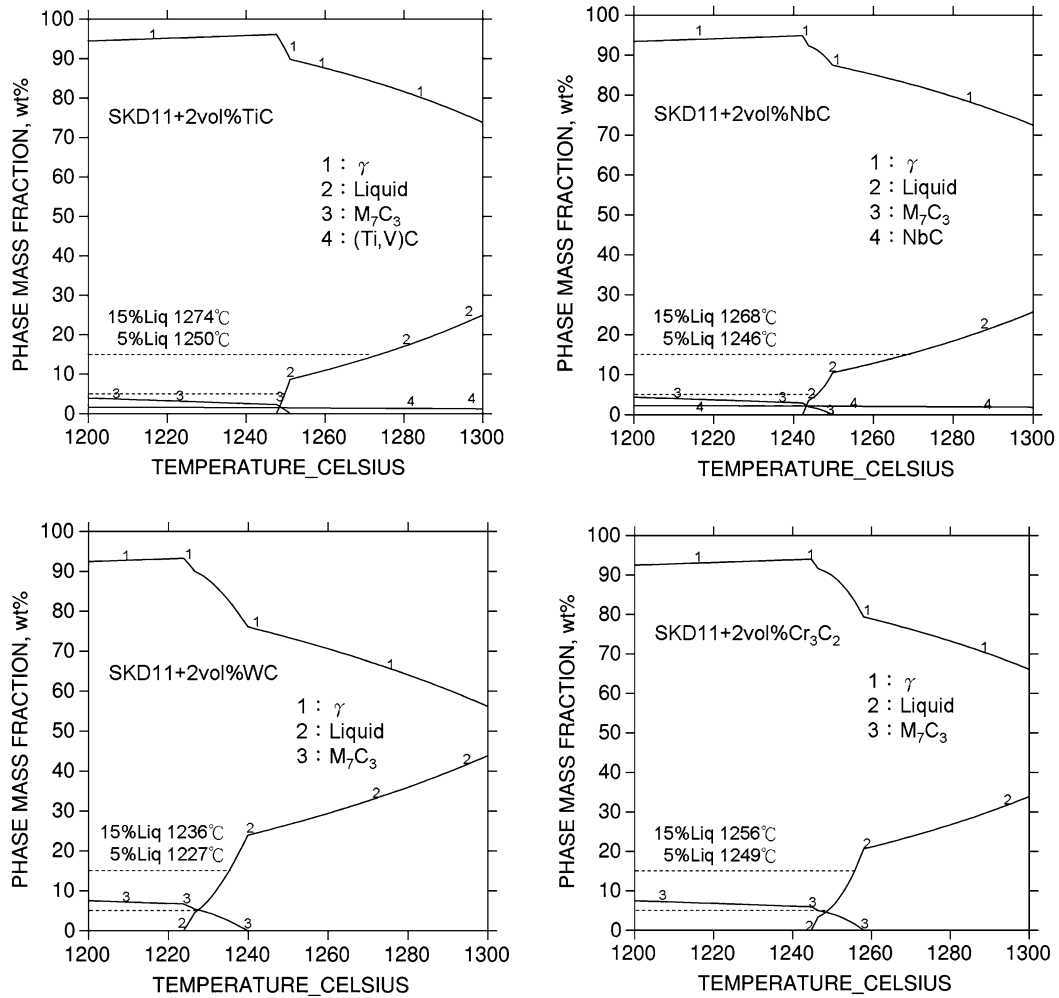


Fig. 14—Amount of liquid, γ , and carbides in SKD11 + 2 vol pct TiC, NbC, WC, and Cr_3C_2 between 1473 and 1573 K (1200 and 1300 °C).

NbC is favored, while WC and Cr_3C_2 are not favored, for shape retention of SKD11. These predictions are in agreement with the experimental results shown in Table IV.

In addition to the preceding two criteria, the particle size and amount of the additives may also play important roles. It is generally accepted that a larger fraction of the second phase and finer particles are more effective in impeding grain growth. It can be argued that the difference in the grain size and the shape retention capability described in the previous sections could have been caused by the different particle sizes of the carbides used. However, Table IV shows that Cr_3C_2 and NbC had similar particle sizes, but NbC performed better. The particle sizes of WC and TiC were also similar, but TiC gave a smaller grain size. This comparison suggests that the particle size may influence the grain growth, but it is not the determining factor.

V. CONCLUSIONS

The challenge of dimensional stability of super-solidus-liquid-phase-sintered SKD11 was alleviated

through the addition of titanium carbide powder. The following are the conclusions drawn from the experimental results and Thermo-Calc calculations.

1. The results of density and distortion of SKD11 indicate that the sintering window is quite narrow, between 1503 and 1513 K (1230 and 1240 °C). The reason is that the temperature range where both liquid and carbide, which act as grain growth inhibitors, exist is quite narrow, as indicated by the phase diagram.
2. Among the TiC, NbC, WC, and Cr_3C_2 examined in this study, TiC is the most effective in impeding grain growth and enlarging the sintering window. With 2 wt pct TiC addition, the sintering window is 1513 to 1553 K (1240 to 1280 °C), broadened from the 10 K of the standard SKD11 to 40 K. Within this temperature range, TiC is retained in the matrix and the grain size is kept smaller than 78 μm .
3. To enlarge the sintering window, an effective carbide must have low solubility in the matrix during sintering and be able to widen the $L + \gamma +$ carbide region in the phase diagram, while the carbide

could be in the original form or in the new carbide form, such as converting from TiC to (Ti,V)C, in this study.

4. Using Thermo-Calc software, effective carbides can be predicted by selecting those that meet the above criteria of low solubility and wide $L + \gamma +$ carbide region. For the four carbides tested in this study, the predictions are in good agreement with the experimental results.

ACKNOWLEDGMENTS

The authors are grateful for the support of this work by the National Science Council of the Republic of China under Contract No. NSC-96-2221-E-002-154-MY2.

REFERENCES

1. H. Berns and A. Saltykova: *Wear*, 2009, vol. 267 (11), pp. 1791–97.
2. N.S. Myers and R.M. German: *Int. J. Powder Metall.*, 1999, vol. 35 (6), pp. 45–51.
3. H. Miura, H. Morikawa, Y. Kawakami, and A. Ishibashi: *J. Jpn. Soc. Powder Metall.*, 1998, vol. 45 (5), pp. 436–41.
4. S. Hachiga and Y. Shiina: *J. Jpn. Soc. Powder Metall.*, 2005, vol. 52 (10), pp. 717–21.
5. H. Nakayama, H. Kyogoku, and S. Komatsu: *J. Jpn. Soc. Powder Metall.*, 2000, vol. 47 (12), pp. 1272–76.
6. H. Kyogoku, S. Komatsu, and H. Nakayama: *J. Jpn. Soc. Powder Metall.*, 1999, vol. 46 (8), pp. 853–57.
7. R.M. German: *Int. J. Powder Metall.*, 1990, vol. 26 (1), pp. 23–34.
8. R. Raman and R.M. German: *Metall. Trans. A*, 1995, vol. 26A, pp. 653–59.
9. R.M. German: *Metall. Mater. Trans. A*, 1997, vol. 28A, pp. 1553–67.
10. G. Herranz, B. Levenfeld, and A. Várez: *Mater. Sci. Forum*, 2007, vols. 534–536 (1), pp. 353–56.
11. C.S. Wright, M. Youseffi, A.S. Wronski, I. Ansara, M. Durand-Charre, J. Mascarenhas, M.M. Oliveira, F. Lemoisson, and Y. Bienvenu: *Powder Metall.*, 1999, vol. 42 (2), pp. 131–46.
12. J. Liu, A. Lal, and R.M. German: *Acta Mater.*, 1999, vol. 47 (18), pp. 4615–26.
13. S. Talacchia, J.I. San Martin, I. Urrutibeaskoa, S. Jauregi, R. Palma, V. Martinez, and J.J. Urcola: *Powder Metall.*, 1993, vol. 36 (4), pp. 275–80.
14. Z. Y. Liu, N.H. Loh, K.A. Khor, and S.B. Tor: *Mater. Sci. Eng. A*, 2001, vol. 311, pp. 13–21.
15. J.D. Bolton and A.J. Gant: *Powder Metall.*, 1997, vol. 40 (2), pp. 143–50.
16. T. Tsuchiyama, S. Takaki, and S. Nakamura: *J. Iron Steel Inst. Jpn.*, 1995, vol. 81 (2), pp. 147–52.
17. G. Herranz, G. Rodriguez, and R. Alonso: *Proc. PM2010 World Congr.*, European Powder Metallurgy Association, Shrewsbury, United Kingdom, 2010, vol. 4, pp. 363–67.
18. J.A. Jiménez, M. Carsí, G. Frommeyer, and O.A. Runao: *Powder Metall.*, 2005, vol. 48 (4), pp. 371–76.
19. S. Weber, W. Theisen, F. Castro, and A. Pyzalla: *Mater. Sci. Eng. A*, 2009, vol. 515, pp. 175–82.
20. C.S. Wright, A.S. Wronski, and I. Iturriza: *Mater. Sci. Technol.*, 2000, vol. 16, pp. 945–57.